THE JOURNAL OF BIOLOGICAL CHEMISTRY Vol. 279, No. 44, Issue of October 29, pp. 45810–45814, 2004
Printed in U.S.A.

Histone H2AX Is Phosphorylated at Sites of Retroviral DNA Integration but Is Dispensable for Postintegration Repair*

Received for publication, July 13, 2004, and in revised form, August 10, 2004
Published, JBC Papers in Press, August 11, 2004, DOI 10.1074/jbc.M407886200

René Daniel‡§¶, Joseph Ramcharan‡§, Emmy Rogakou‖, Konstantin D. Taganov‡ ‡‡, James G. Greger‡, William Bonner‖, André Nussenzweig§§, Richard A. Katz‡, and Anna Marie Skalka‡¶¶**

From the ‡Fox Chase Cancer Center, Institute for Cancer Research, Philadelphia, Pennsylvania 19111-2497, ‖Laboratory of Molecular Pharmacology, NCI, National Institutes of Health, Bethesda, Maryland 20892, and §§Experimental Immunology Branch, NCI, National Institutes of Health, Bethesda, Maryland 20892

The histone variant H2AX is rapidly phosphorylated (denoted γH2AX) in large chromatin domains (foci) flanking double strand DNA (dsDNA) breaks that are produced by ionizing radiation or genotoxic agents and during V(D)J recombination. H2AX-deficient cells and mice demonstrate increased sensitivity to dsDNA break damage, indicating an active role for γH2AX in DNA repair; however, γH2AX formation is not required for V(D)J recombination. The latter finding has suggested a greater dependence on γH2AX for anchoring free broken ends *versus* ends that are held together during programmed breakage-joining reactions. Retroviral DNA integration produces a unique intermediate in which a dsDNA break in host DNA is held together by the intervening viral DNA, and such a reaction provides a useful model to distinguish γH2AX functions. We found that integration promotes transient formation of γH2AX at retroviral integration sites as detected by both immunocytological and chromatin immunoprecipitation methods. These results provide the first direct evidence for the association of newly integrated viral DNA with a protein species that is an established marker for the onset of a DNA damage response. We also show that H2AX is not required for repair of the retroviral integration intermediate as determined by stable transduction. These observations provide independent support for an anchoring model for the function of γH2AX in chromatin repair.

The evolutionarily conserved histone H2AX comprises approximately 2–25% of the histone H2A pool in mammalian cells and is incorporated randomly into nucleosomes (1). The extended C-terminal tail of H2AX contains a serine (Ser-139) embedded in an invariant SQE motif that is a target for phosphorylation by the phosphatidylinositol 3-kinase-related DNA-PK, ataxia-telangiectasia-mutated (ATM), and ATM and Rad3-related (ATR) protein kinases (2–4). This H2AX serine residue is massively and rapidly phosphorylated at sites of double strand breaks (DSBs)[1] and stalled replication forks (3, 5, 6), forming microscopically visible foci on staining with a specific antibody. This phosphorylation seems to play an important role in processing or repair of DSBs (7, 8). H2AX phosphorylation has also been observed at sites of V(D)J recombination (9), meiotic strand breaks, and other physiologically programmed reactions in which DSBs are formed (10–12).

Early events in retroviral replication include entry of the viral capsid with the accompanying enzymes reverse transcriptase and integrase (IN) followed by synthesis of a DNA copy of the viral RNA genome to form a preintegration complex. This complex then enters the nucleus, and integration is first detected at approximately 3–4 h postinfection (13). Retroviral integration is catalyzed by integrase acting on specific sequences at the ends of the viral DNA and via a concerted cleavage-ligation reaction that is mechanistically similar to that catalyzed by RAG proteins during V(D)J recombination (14–16) (Fig. 1*A*). As a consequence of integrase-mediated joining, the host cell DNA suffers a DSB, but the ends are held together by single strand links to viral DNA (Fig. 1*B*). Postintegration repair of this intermediate (Fig. 1*B*) is essential for the maintenance of host DNA integrity as well as the stable association of retroviral DNA with host chromosomes. Numerous lines of evidence (17–20) indicate that retroviral DNA elicits a DNA damage response and that the integration intermediate is repaired primarily via components of the non-homologous end-joining (NHEJ) pathway. In this study, we asked whether H2AX is phosphorylated at sites of retroviral DNA integration and whether this response is essential for repair of this complex lesion as determined by survival of stably transduced cells.

EXPERIMENTAL PROCEDURES

Cells and Viruses—MO59K cells (purchased from American Type Culture Collection) were maintained as described previously (18, 19), and mouse embryonic fibroblasts (MEFs) were maintained as described

* This work was supported by National Institutes of Health Grants AI40385, CA71515, CA98090, and CA06927, a Tobacco Formula Research Fund Grant from the Pennsylvania Department of Health, and by an appropriation from the Commonwealth of Pennsylvania. The costs of publication of this article were defrayed in part by the payment of page charges. This article must therefore be hereby marked "*advertisement*" in accordance with 18 U.S.C. Section 1734 solely to indicate this fact.

§ These authors contributed equally to this work.
¶ Present address: Thomas Jefferson University, 1020 Walnut St., Philadelphia, PA 19107-5587.
** Present address: Inst. of Molecular Biology and Genetics, Biomedical Sciences Research Center "Al. Fleming," 34 Al. Fleming St., Vari-Athens 16602, Greece.
‡‡ Present address: California Institute of Technology, Pasadena, CA 91125.
¶¶ To whom correspondence should be addressed: Fox Chase Cancer Center, 333 Cottman Ave., Philadelphia, PA 19111-2497. Tel: 215-728-2490; Fax: 215-728-2778; E-mail: AM_skalka@fccc.edu.

[1] The abbreviations used are: DSB, double strand break; IN, integrase; ASV, avian sarcoma virus; HIV, human immunodeficiency virus; m.o.i., multiplicity of infection; ChIP, chromatin immunoprecipitation; PIPES, 1,4-piperazinediethanesulfonic acid; NHEJ, non-homologous end-joining; EGFP, enhanced green fluorescent protein; VSV, vesicular stomatitis virus; MEFs, mouse embryonic fibroblasts.

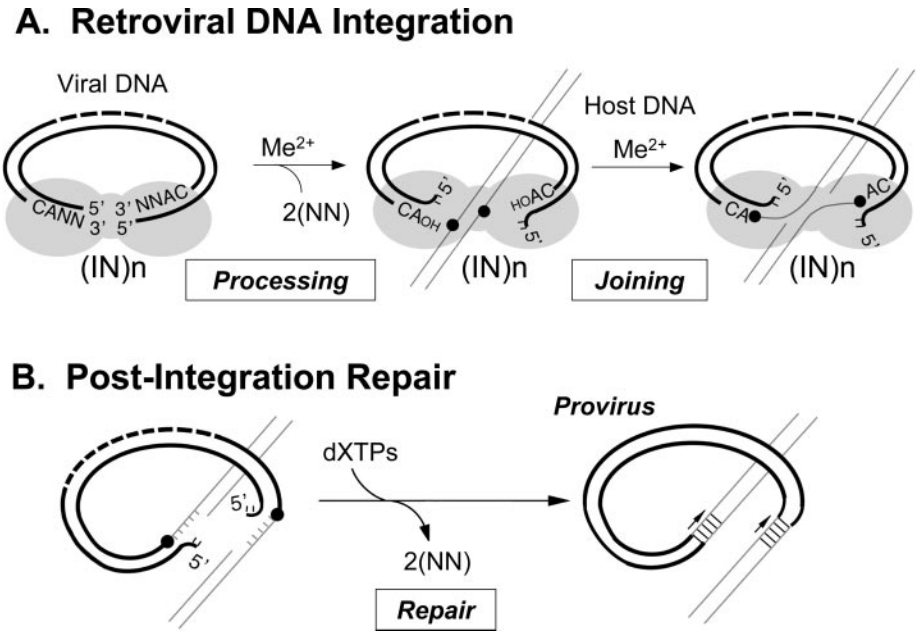

FIG. 1. **Stable, heritable establishment of a retroviral provirus requires integrase-mediated DNA integration and postintegration repair of the integration intermediate by host proteins.** *A*, the first two steps in this process are catalyzed by a multimer of integrase, (*IN*)*n*. *B*, postintegration repair is dependent on host cell functions.

previously (17). The ASV-based vectors IN^+ and IN^- and the HIV-1-based vector were described previously (17, 19).

Immunofluorescence and Quantification of Foci—Cells were plated and infected the following day at multiplicity of infection (m.o.i.) 10. The cells were washed with phosphate-buffered saline and fixed with 4% paraformaldehyde at the indicated times postinfection. After permeabilization with 0.2% Triton X-100, samples were blocked overnight with 3% bovine serum albumin at 4 °C. The slides were incubated with a mouse monoclonal antibody against γH2AX (Upstate) and then with Alexa Fluor 488 conjugated goat anti-mouse IgG (Molecular Probes) as secondary antibody. Nuclei were stained with 4,6-diamidino-2-phenylindole prior to mounting the slides with SlowFade antifade reagent (Molecular Probes).

Processed cells were examined for γH2AX foci by monitoring fluorescence of the Alexa Fluor dye using an UltraView confocal imaging system (PerkinElmer Life Sciences) in which the confocal scanning head was mounted on a Nikon TE-200E microscope. Optical sections along the *z* axis of the nuclei were captured at 0.1-μm intervals, and the final images were obtained by projection of the individual sections. For each time point, images of at least 100 cells were captured and used for quantitative analysis of γH2AX foci. To prevent bias in the selection of cells that displayed foci, nuclei were randomly selected for 4,6-diamidino-2-phenylindole staining and then monitored for focus formation. The γH2AX foci were counted in each cell using Image-Pro Plus (Media Cybernetics). A setting that excluded relatively weak foci and background speckles was used as a standard for foci quantitation in all the cells selected for analysis.

A simple stochastic model for viral integration and formation of γH2AX foci was designed to relate the number of foci counted in cells to the time of observation. Virus is modeled as being integrated at 4 h, on average, after the start of the experiment. The exact time of integration and start of H2AX phosphorylation are taken to be normally distributed, with a mean of 4 h and a standard deviation of 1.1 h. H2AX phosphorylation is modeled to continue for an exponentially distributed random time, with a mean of 2.6 h. The number of viruses integrating in a cell is taken to be Poisson distributed. The best fit to experimental data is achieved with a mean m.o.i. of 8.5 viruses/cell.

Chromatin Immunoprecipitation—Chromatin immunoprecipitation (ChIP) assays were performed as described by Boyd and Farnham (21). In our experiments, 10^6 HeLa cells were infected with amphotropic ASV vectors IN^+ or IN^- (17). At defined times after infection, formaldehyde (1% final) was added, and the cultures were incubated at room temperature for 30 min to cross-link viral DNA and interacting proteins. The cross-linking reaction was quenched with glycine (0.125 M final concentration). Plates were washed with cold 1× phosphate-buffered saline, and then cells were scraped into 1× phosphate-buffered saline that contained protease inhibitors and washed and lysed by addition of 0.5% Nonidet P-40, 5 mM PIPES, pH 8.0, 85 mM KCl, and protease inhibitors. The intact nuclei were isolated by centrifugation at 5000 rpm at 4 °C. Nuclei were then resuspended in a lysis buffer (1% SDS, 50 mM Tris-Cl, pH 8.1, 10 mM EDTA, protease inhibitors). Chromatin was sonicated to fragments containing DNA of an average length of approximately 600 bp. Samples were subjected to centrifugation to remove debris and were precleared by shaking for 1 h with salmon sperm DNA/protein A-agarose (Upstate). After removal of the salmon sperm DNA/protein A-agarose, supernatants were diluted 10-fold with a dilution buffer (0.01% SDS, 1.1% Triton X-100, 1.2 mM EDTA, 16.7 mM Tris-Cl, pH 8.1, 167 mM NaCl, protease inhibitors), and chromatin fragments were immunoprecipitated overnight with antibodies to ASV integrase (rabbit polyclonal), γH2AX (mouse monoclonal) (Upstate), and phosphatidylinositol 3-kinase p110 (mouse monoclonal) (Santa Cruz Biotechnology) proteins. Protein-DNA-antibody complexes were isolated by the addition of salmon sperm DNA/protein A-agarose. After 1 h, complexes were collected by centrifugation and washed three times with a wash buffer (100 mM Tris, pH 8, 500 mM LiCl, 1% Nonidet P-40, 1% deoxycholic acid). Pellets were eluted with 50 mM $NaHCO_3$, 1% SDS for 15 min at room temperature. Clarified samples were incubated with RNase and 5 M NaCl at 67 °C for 4–5 h to reverse cross-links and then precipitated overnight with ethanol. Following centrifugation, pellets were resuspended in proteinase K buffer and treated with proteinase K. After phenol/chloroform extraction, the DNA was precipitated with ethanol. Viral sequences in these fractions were detected by PCR using primers targeting the long terminal repeats. The sequence of the left primer was 5′-ACG TCC AGG GCC CGG AGC GAC-3′, and the right primer was 5′-CTT CAA TGC CCC CAA AAC CAA-3′. PCR products were resolved by electrophoresis on an agarose gel and subjected to Southern blotting with a radioactive probe against the ASV long terminal repeat (generated by using random primers and a PCR fragment made with the long terminal repeat probe primers 5′-GAT TGG TGG AAG TAA GGT GG-3′ and 5′-CAA ATG GCG TTT ATT GTA TCG-3′). As a negative control, we used primers targeting the cellular p21 promoter sequences, left, 5′-TTT CCA CCT TTC ACC ATT CC-3′, and right, 5′-GGC AGA TCA CAT ACC CTG TT-3′, with a probe generated by using random primers.

Transduction Assays—For infection with the ASV vector (22), MEFs were plated at a density of 10^5 cells/60-mm dish. On the following day, cells were infected in the presence of 5 μg/ml DEAE-dextran. At 8 days postinfection, EGFP-positive cells were counted by flow cytometry. For infection with the HIV-1 vector, MEFs were plated at a density of 5×10^4 cells/well in a 24-well plate. The following day, cells were infected with an HIV-1 EGFP vector (23). Transduced cells were counted by flow cytometry as with the ASV vector.

RESULTS

To determine whether retroviral infection induces formation of γH2AX foci, we infected cells with an amphotropic ASV vector (17) and examined them by immunofluorescence with an antibody specific for γH2AX. In preliminary experiments (data not included), we observed the formation of γH2AX foci early after infection in DNA repair-proficient human (HeLa and

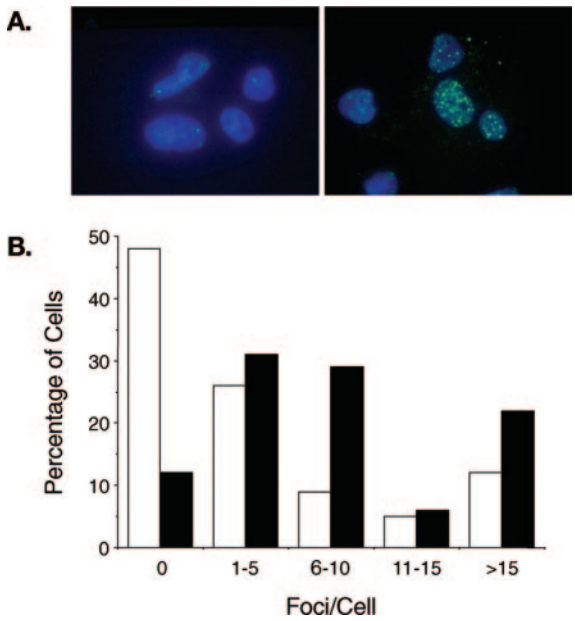

FIG. 2. **Retroviral infection induces formation of γH2AX foci.** *A*, confocal images show uninfected MO59K cells (*left*) and 6 h postinfection with an ASV vector at m.o.i. 10 (*right*). Nuclei were stained with 4,6-diamidino-2-phenylindole (*blue*). *B*, distribution of foci is shown in uninfected cells (*open bars*) and in cells 6 h after infection (*filled bars*).

MO59K) and mouse (3T3) cells. As a control, we infected cells with an integration-deficient (IN^-) vector (17), and no increase in foci over background was detected. The data in Fig. 2 and Table I summarize results from subsequent experiments, which included computer-assisted quantitative analyses of γH2AX foci in MO59K cells infected at m.o.i. 10 infectious particles/cell. We again observed an increased number of foci in the infected culture (Fig. 2*A*), which appeared to peak at 6 h postinfection. A comparison of the distribution of the number of foci/cell in uninfected cells with the number of foci/cell 6 h postinfection is shown in Fig. 2*B*. The bulk (~75%) of the uninfected cells contained no or few foci/cell, whereas a small proportion (~10%) displayed numerous foci, which we speculate may have been caused by replication stress; such cells were also observed in the infected culture. At 6 h postinfection, the infected culture had many fewer cells with no foci, and the percentage of cells with 5–10 foci was substantially higher than in the uninfected culture. As summarized in Table I, this value increased sharply by 4 h postinfection, when integration is expected to begin. The average number of virus-induced foci peaked at 5.1 foci/cell in the 6-h sample and declined again at 8 h postinfection. γH2AX foci are reported (6) to arise within minutes at sites of DNA damage and start to disappear after 30 min, with an ~2-h half-life as damage is repaired. Assuming similar kinetics, it is likely that some integration-induced foci were both formed and resolved within the 8-h interval monitored in this experiment. A computer simulation using such parameters produced data consistent with the numbers of virus-induced foci/cell in a culture infected at m.o.i. ~10, at the postinfection time points shown in Table I.

To verify that H2AX is phosphorylated at sites of retroviral DNA integration, we immunoprecipitated chromatin from nuclear extracts with a γH2AX-specific antibody (ChIP assay) and screened for the presence of viral DNA using PCR. To test the feasibility of this approach, ChIP was first performed at 6 h postinfection of HeLa cells at m.o.i. 0.001, 0.01, or 0.1 infectious particles/cell (Fig. 3*A*, *lanes 2–4*). As expected, antibody specific for integrase protein (positive control) precipitated viral DNA in this extract and in amounts proportional to the m.o.i. An

TABLE I
Quantitative assessment of γH2AX foci formation in response to retroviral infection in MO59K cells

Cells were infected at an m.o.i. of 10, fixed with paraformaldehyde at the indicated times following infection, and immunostained with γH2AX antibody. The number of foci/cell as well as the percentage of cells displaying foci for an 8-h time course postinfection were determined as described under "Experimental Procedures." The number of virus-induced foci/cell was determined by subtracting the background foci in uninfected cells (time 0) from the various time points.

Time postinfection	Percentage of cells with foci	No. of foci/cell	No. of virus induced foci/cell
h			
0	53	5.2	0.0 (0.00)[a]
2	51	5.5	0.3 (0.26)
4	92	8.6	3.4 (3.41)
6	88	10.3[b]	5.1 (4.88)
8	84	8.2	3.0 (3.05)

[a] The numbers in parentheses are from the computer simulation described under "Experimental Procedures."
[b] $p < 10^{-6}$ for this time point.

association of viral DNA with the γH2AX immunoprecipitate was also readily detected and, as with integrase, in proportion to the m.o.i. Approximately 10% of the viral DNA was coimmunoprecipitated with γH2AX in this test. Based on the calculated efficiency of the antibody used for these analyses (data not shown), the actual amount of nuclear viral DNA associated with γH2AX in this experiment is estimated to be ~37% of the total. No association of viral DNA was detected with the phosphatidylinositol 3-kinase antibody (negative control). In addition, none of the antibodies precipitated sequences corresponding to a region in the cellular p21 promoter (DNA negative control). In this experiment, viral DNA was quantified by Southern blot, but comparable results were obtained with real time PCR (not shown). Because results with m.o.i. 0.1 are clearly in the titratable range for ChIP analysis, this was the condition adopted in the two separate experiments summarized in Fig. 3, *B* and *C*. Fig. 3*B* shows results of ChIP analyses following infection with integration-competent (IN^+) or integration-defective (IN^-) ASV vectors. A peak of association of γH2AX and viral DNA was observed in the IN^+ infection at 6 h postinfection, and no association was detected after infection with the IN^- vector. This result demonstrates that γH2AX is associated with nuclear viral DNA only after this DNA is integrated into chromatin.

To examine more closely the kinetics of accumulation of γH2AX at integration sites, the amount of viral DNA captured by ChIP at 2-h intervals was determined up to 16 h postinfection (Fig. 3*C*). Values for each time point were expressed as a percentage of the total viral DNA in the nuclear fraction that is associated with the ChIP at each time, corrected for immunoprecipitation efficiency of the γH2AX antibody. Consistent with our analysis of foci in infected MO59K cells (Table I), these results showed that an association with γH2AX peaks at ~6 h, shortly after viral DNA is detected in the nuclear extract. We estimate that 60% of the nuclear viral DNA in this experiment is associated with γH2AX and therefore is integrated at this time point. From these results, we conclude that γH2AX is a valid marker for sites of retroviral DNA integration. We note that ChIP detects integrated viral DNA both before and after repair (Fig. 1). To examine the functional relevance of H2AX phosphorylation to repair, we performed the transduction assays described below.

Because transduced genes are expressed efficiently only from stably integrated proviruses, retroviral transduction is a readout for successful postintegration repair. For example, we have shown that the transduction efficiency of NHEJ-defective DNA-PKcs-deficient murine cells is reduced by 80–90% com-

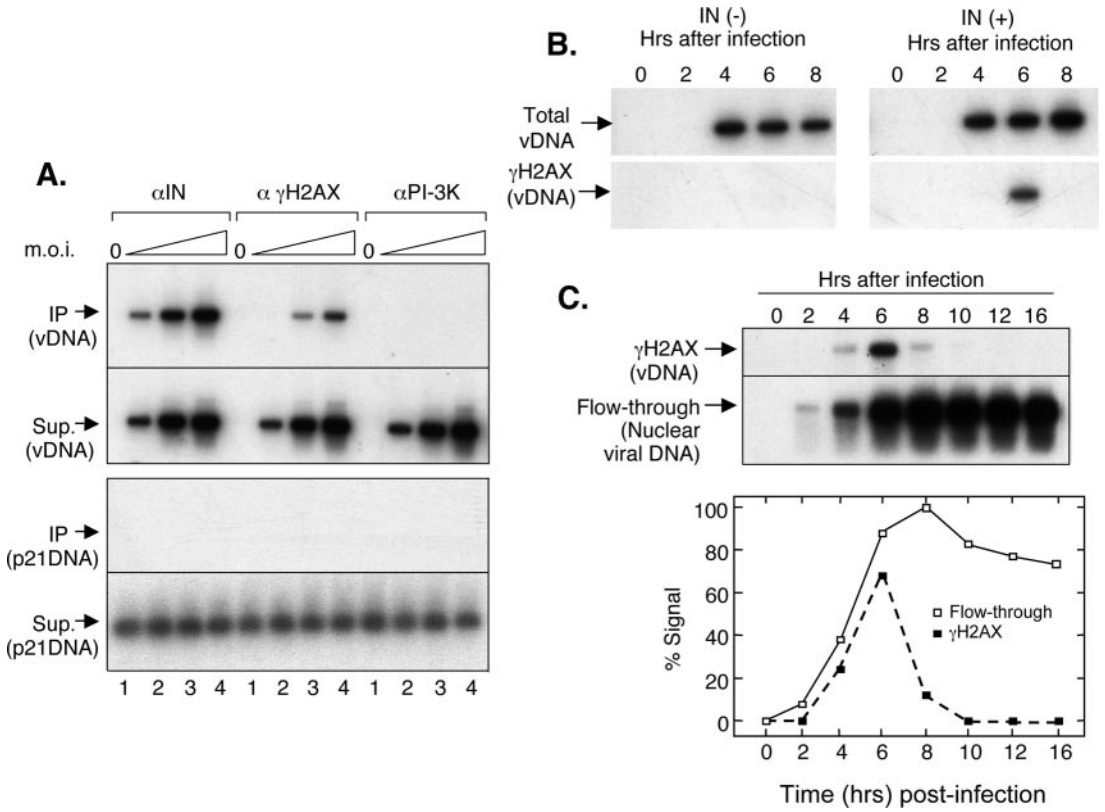

FIG. 3. **Association of viral DNA with γH2AX.** HeLa cells were infected and chromatin immunoprecipitation (*IP*) was performed as described under "Experimental Procedures." *A*, results are shown with nuclear lysates from cells at 6 h after infection with the ASV vector at m.o.i. 0.001, 0.01, or 0.1. *PI-3K*, phosphatidylinositol 3-kinase. *Sup.*, supernatant. *B*, results are shown of γH2AX ChIP assays with cells infected with the IN^+ and IN^- ASV vectors at m.o.i. 0.1. *C*, time course of association of γH2AX with integrated viral DNA after infection at m.o.i. 0.1 is shown.

TABLE II
Transduction efficiency of H2AX null cells and null cells complemented with H2AX genes carrying mutation of the C-terminal phosphorylation site of this histone

Cells were infected with an amphotropic ASV vector carrying an EGFP reporter (23). Virus titer ~1.4×10^5 infectious particles/ml. wt, wild type.

Virus dilution	EGFP-positive cells				
	H2AX+/+	H2AX−/−	H2AX−/− + wt H2AX	H2AX−/− + S136A/S139A	H2AX−/− + S136E/S139E
	%	%	%	%	%
10^{-3}	66.3	62.0	59.1	74.1	64.1
10^{-4}	14.1	12.1	11.6	15.2	16.0
10^{-5}	1.8	1.2	1.1	1.7	1.6

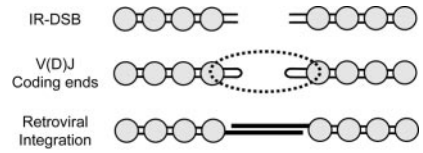

FIG. 4. **Broken chromosomal ends may be held together by several mechanisms to facilitate NHEJ.** Proximity of ends produced by ionizing radiation (*IR*) or treatment with genotoxic agents would be enhanced by γH2AX-mediated anchoring via specific protein-protein interactions. Ends produced during V(D)J recombination would also be held together by the RAG1/2 protein complex (*dashed oval*). Ends produced during retroviral integration are linked by single stand covalent bonds to viral DNA and, perhaps, by the viral IN complex as well.

pared with wild type cells or deficient cells into which DNA-PKcs-expressing DNA was reintroduced (17, 20). As the DNA damage induced by integration cannot be repaired efficiently, most NHEJ-deficient cells are unlikely to survive infection and therefore cannot give rise to stable transductants. To find out whether H2AX phosphorylation is required for postintegration repair, we performed transduction experiments using MEF lines obtained from H2AX knock-out mice and derivatives (24, 25), and the ASV-EGFP vector. Results in Table II show that there is no significant difference between the transduction efficiency with H2AX+/+ and H2AX−/− MEFs. Similar results were obtained with a VSV-G protein-pseudo-typed HIV-1 GFP vector (not shown). These data indicate that H2AX deficiency has little or no effect on postintegration repair. One possible explanation for this result is that H2AX function in these cells is redundant. We therefore examined transduction in H2AX−/− MEFs that had been complemented with transgenes that express wild type murine H2AX or proteins carrying either neutral non-modifiable substitutions (S136A/S139A) or negatively charged substitutions that mimic constitutive phosphorylation (S136E/S139E) in the C-terminal phosphatidylinositol 3-kinase-related protein kinase target sites of H2AX. No significant difference was observed between the efficiencies of transduction of these lines compared with H2AX−/− cells (Table I). It appears, therefore, that H2AX phosphorylation is dispensable for postintegration repair.

DISCUSSION

In this study, we show that retroviral infection induces the formation of histone γH2AX foci, and chromatin immunoprecipitation assays confirmed that H2AX phosphorylation occurs at sites of retroviral DNA integration. Therefore, these results are consistent with our previous findings (17–20) that cells respond to retroviral DNA integration in a manner similar to DSBs. We also demonstrate that an H2AX deficiency and an inability to phosphorylate this histone have no detectable effect on the efficiency of retroviral transduction of cultured mouse cell lines. Because efficient expression of transduced genes

requires stable retroviral vector integration, we conclude that H2AX phosphorylation is largely dispensable for postintegration repair of chromatin damage.

Although γH2AX is required for the accumulation of a subset of repair and signaling proteins into irradiation-induced foci (7, 8, 24, 26, 27), the exact role of H2AX phosphorylation is not well understood. Some DNA damage-sensing and repair proteins have been shown to interact physically with γH2AX (27–29). A functional role for γH2AX has been indicated because H2AX-deficient cells are hypersensitive to ionizing radiation, exhibit genomic instability, and also show an aberrant checkpoint response under certain conditions (7, 8, 30). On the other hand, although γH2AX foci form at sites of V(D)J recombination, H2AX appears to be dispensable for this reaction when tested with extrachromosomal substrates in cultured cells (7, 8, 30).

The study of H2AX-deficient mice has provided further insight into H2AX function. H2AX mice are viable, but DNA repair seems to proceed less efficiently in such animals, which show modest sensitivity to ionizing radiation and impairment in immunoglobulin class-switch recombination (31). In keeping with results from the cell-based assays cited above, these mice show no detectable abnormalities in V(D)J recombination (7, 8). However, the genomic caretaker function of H2AX is more fully exposed when cell cycle checkpoints are compromised because of the absence of p53 (25, 32). In a p53−/− background, even H2AX+/− heterozygotes show increased misrepair of DNA damage, leading to the development of immature T- and B-cell lymphomas and solid tumors. Some of the B-cell lymphomas harbor oncogenic translocations with hallmarks of aberrant V(D)J recombination. It appears therefore that, although H2AX is not required for V(D)J recombination, it can suppress misrepair of RAG-dependent DSBs. Based on these and other observations, two general, non-exclusive models have been proposed for γH2AX function. 1) The high concentration of repair proteins recruited to the vicinity of DSBs by or through some action of γH2AX may facilitate repair, especially at low (threshold) levels of damage (30); or 2) γH2AX interaction with such proteins might help to hold broken ends together, thereby minimizing the risk of misrepair (25, 32–34). According to these models, differential dependency on H2AX is expected, with more dependence on γH2AX for the repair of free DSBs formed by ionizing radiation than for programmed recombination reactions (*e.g.* V(D)J), in which ends are held in proximity by recombination proteins (35). H2AX−/− spermatocytes show severe defects in meiotic X-Y chromosome pairing (12), and as such, it is tempting to speculate that γH2AX plays a bridging function during meiotic recombination.

In summary, our studies have produced two important findings. First, they provide direct confirmation that cultured cells respond to retroviral DNA integration in the same way that they respond to DSBs produced by a variety of genotoxic agents or normal programmed events, namely, by massive phosphorylation of histone H2AX in the vicinity of the damage site. The second finding is that H2AX appears to be dispensable for postintegration repair. These observations lend independent support to a model in which the anchoring of broken DNA ends to facilitate their repair is a critical function of γH2AX. Because chromosome breaks are likely to be held together by the RAG1/2 complex during V(D)J recombination and are held covalently by viral DNA in retroviral integration (Fig. 4), such an anchoring function should not be essential in either reaction.

Acknowledgments—We thank Dr. Samuel Litwin for performing the computer simulations summarized in Table I and the following Fox Chase Cancer Center Shared Facilities used in the course of this work: Cell Imaging Facility, Biostatistics Facility, and Research Secretarial Services.

REFERENCES

1. Rogakou, E. P., Pilch, D. R., Orr, A. H., Ivanova, V. S., and Bonner, W. M. (1998) *J. Biol. Chem.* **273,** 5858–5868
2. Burma, S., Chen, B. P., Murphy, M. B., Kurimasa, A., and Chen, D. J. (2001) *J. Biol. Chem.* **276,** 42462–42467
3. Ward, I. M., and Chen, J. (2001) *J. Biol. Chem.* **276,** 47759–47762
4. Stiff, T., O'Driscoll, M., Rief, N., Iwabuchi, K., Lobrich, M., and Jeggo, P. A. (2004) *Cancer Res.* **64,** 2390–2396
5. Rogakou, E. P., Boon, C., Redon, C., and Bonner, W. M. (1999) *J. Cell Biol.* **146,** 905–916
6. Redon, C., Pilch, D., Rogakou, E., Sedelnikova, O., Newrock, K., and Bonner, W. (2002) *Curr. Opin. Genet. Dev.* **12,** 162–169
7. Celeste, A., Petersen, S., Romanienko, P. J., Fernandez-Capetillo, O., Chen, H. T., Sedelnikova, A. O., Reina-San-Martin, B., Coppola, V., Meffre, E., Difilippantonio, M. J., Redon, C., Pilch, D. R., Olaru, A., Eckhaus, M., Camerini-Otero, D. C., Tessarollo, L., Livak, F., Manova, K., Bonner, W. M., Nussenzweig, M. C., and Nussenzweig, A. (2002) *Science* **296,** 922–927
8. Bassing, C. H., Chua, K. F., Sekiguchi, J., Suh, H., Whitlow, S. R., Fleming, J. C., Monroe, B. C., Ciccone, D. N., Yan, C., Vlasakova, K., Livingston, D. M., Ferguson, D. O., Scully, R., and Alt, F. W. (2002) *Proc. Natl. Acad. Sci. U. S. A.* **99,** 8173–8178
9. Chen, H. T., Bhandoola, A., Difilippantonia, M. J., Zhu, J., Brown, M. J., Tai, X., Rogakou, E. P., Brotz, T. M., Bonner, W. M., Ried, T., and Nussenzweig, A. (2000) *Science* **290,** 1962–1965
10. Petersen, S., Casellas, R., Reina-San-Martin, B., Chen, H. T., Difilippantonio, M. J., Wilson, P. C., Hanitsch, L., Celeste, A., Muramatsu, M., Pilch, D. R., Redon, C., Ried, T., Bonner, W. M., Honjo, T., Nussenzweig, M. C., and Nussenzweig, A. (2001) *Nature* **414,** 660–665
11. Mahadevaiah, S. K., Turner, J. M., Baudat, F., Rogakou, E. P., de Boer, P., Blanco-Rodriguez, J., Jasin, M., Keeney, S., Bonner, W. M., and Burgoyne, P. S. (2001) *Nat. Genet.* **27,** 271–276
12. Fernandez-Capetillo, O., Mahadevaiah, S. K., Celeste, A., Romanienko, P. J., Camerini-Otero, R. D., Bonner, W. M., Manova, K., Burgoyne, P., and Nussenzweig, A. (2003) *Dev. Cell* **4,** 497–508
13. Vandegraaff, N., Kumar, R., and Burrell, C. J. (2001) *J. Virol.* **75,** 11253–11260
14. Katz, R. A., and Skalka, A. M. (1994) *Annu. Rev. Biochem.* **63,** 133–173
15. Craig, N. L. (1996) *Science* **271,** 1512
16. van Gent, D. C., Mizuuchi, K., and Gellert, M. (1996) *Science* **271,** 1592–1594
17. Daniel, R., Katz, R. A., and Skalka, A. M. (1999) *Science* **284,** 644–647
18. Daniel, R., Katz, R. A., Merkel, G., Hittle, J. C., Yen, T. J., and Skalka, A. M. (2001) *Mol. Cell. Biol.* **21,** 1164–1172
19. Daniel, R., Kao, G., Taganov, K., Greger, J., Favorova, O., Merkel, G., Yen, T. J., Katz, R. A., and Skalka, A. M. (2003) *Proc. Natl. Acad. Sci. U. S. A.* **100,** 4778–4783
20. Daniel, R., Greger, J., Katz, R. A., Taganov, K., Wu, X., Kappes, J. C., and Skalka, A. M. (2004) *J. Virol.* **78,** 8573–8581
21. Boyd, K. E., and Farnham, P. J. (1999) *Mol. Cell. Biol.* **19,** 8393–8399
22. Katz, R. A., Greger, J. G., Boimel, P., and Skalka, A. M. (2003) *J. Virol.* **77,** 13412–13417
23. Katz, R. A., Greger, J. G., Darby, K., Boimel, P., Rall, G. F., and Skalka, A. M. (2002) *J. Virol.* **76,** 5422–5434
24. Celeste, A., Fernandez-Capetillo, O., Kruhlak, M. J., Pilch, D. R., Staudt, D. W., Lee, A., Bonner, R. F., Bonner, W. M., and Nussenzweig, A. (2003) *Nat. Cell Biol.* **5,** 675–679
25. Celeste, A., Difilippantonio, S., Difilippantonio, M. J., Fernandez-Capetillo, O., Pilch, D. R., Sedelnikova, O. A., Eckhaus, M., Ried, T., Bonner, W. M., and Nussenzweig, A. (2003) *Cell* **114,** 371–383
26. Paull, T. T., Rogakou, E. P., Yamazaki, V., Kirchgessner, C. U., Gellert, M., and Bonner, W. M. (2000) *Curr. Biol.* **10,** 886–895
27. Stewart, G. S., Wang, B., Bignell, C. R., Taylor, A. M., and Elledge, S. J. (2003) *Nature* **421,** 961–966
28. Ward, I. M., Minn, K., Jorda, K. G., and Chen, J. (2003) *J. Biol. Chem.* **278,** 19579–19582
29. Kobayashi, J., Tauci, H., Sakamoto, S., Nakamura, A., Morishima, K., Matsuura, S., Kobayashi, T., Tamai, K., Tanimoto, K., and Komatsu, K. (2002) *Curr. Biol.* **12,** 1846–1851
30. Fernandez-Capetillo, O., Chen, H. T., Celeste, A., Ward, I. M., Romanienko, P. J., Morales, J. C., Naka, K., Xia, Z., Camerini-Otero, R. D., Motoyama, N., Carpenter, P. B., Bonner, W. M., Chen, J., and Nussenweig, A. (2002) *Nat. Cell Biol.* **4,** 993–997
31. Reina-San-Martin, B., Difilippantonio, S., Hanitsch, L., Masilamani, R. F., Nussenzweig, A., and Nussenzweig, M. C. (2003) *J. Exp. Med.* **197,** 1767–1778
32. Bassing, C. H., Suh, H., Ferguson, D. O., Chua, K. F., Manis, J., Eckersdorff, M., Gleason, M., Bronson, R., Lee, C., and Alt, F. W. (2003) *Cell* **114,** 359–370
33. Bassing, C. H., and Alt, F. W. (2004) *Cell Cycle* **3,** 149–153
34. Fernandez-Capetillo, O., Lee, A., Nussenzweig, M. C., and Nussenzweig, A. (2004) *DNA Repair* (*Amst.*) **3,** 959–967
35. Jones, J. M., and Gellert, M. (2003) *Proc. Natl. Acad. Sci. U. S. A.* **100,** 15446–15451